Printed in the Republic of Korea

ANALYTICAL SCIENCE & TECHNOLOGY

Vol. 36 No. 5, 236-249, 2023

https://doi.org/10.5806/AST.2023.36.5.236

Morphological study of porous aromatic schiff bases as a highly effective carbon dioxide storages

Rehab Hammoda[1], Naser Shaalan[1], Mohammed H. Al-Mashhadani[2], Dina S. Ahmed[3], Rahimi M. Yusop[4], Ali H. Jawad[5], and Emad Yousif[2,★]

[1]Department of Chemistry, College of Science for Women, University of Baghdad, Iraq
[2]Department of Chemistry, College of Science, Al-Nahrain University, P. O. Box: 64021, Baghdad, Iraq
[3]Department of Chemical Industries, Institute of Technology-Baghdad, Middle Technical University, Baghdad, Iraq
[4]School of Chemical Science, Faculty of Science and Technology, University Kebangsaan Malaysia, 43600 Bangi, Selangor, Malaysia
[5]Faculty of Applied Sciences, Universiti Teknologi MARA, Shah Alam 40450, Selangor, Malaysia

(Received April 29, 2023; Revised June 14, 2023; Accepted June 26, 2023)

Abstract: Carbon dioxide (CO_2) capture and storage is a critical issue for mitigating climate change. Porous aromatic Schiff base complexes have emerged as a promising class of materials for CO_2 capture due to their high surface area, porosity, and stability. In this study, we investigate the potential of Schiff base complexes as an effective media for CO_2 storage. We review the synthesis and characterization of porous aromatic Schiff bases materials complexes and examine their CO_2 sorption properties. We find that Schiff base complexes exhibit high CO_2 adsorption capacity and selectivity, making them a promising candidate for use in carbon capture applications. Moreover, we investigate the effect of various parameters such as temperature, and pressure on the CO_2 adsorption properties of Schiff base complexes. The Schiff bases possessed tiny Brunauer-Emmett-Teller surface areas (4.7-19.4 m^2/g), typical pore diameters of 12.8-29.43 nm, and pore volumes ranging from 0.02-0.073 cm^3/g. Overall, our results suggest that synthesized complexes have great potential as an effective media for CO_2 storage, which could significantly reduce greenhouse gas emissions and contribute to mitigating climate change. The study provides valuable insights into the design of novel materials for CO_2 capture and storage, which is a critical area of research for achieving a sustainable future.

Key words: greenhouse gases, surface morphology, porous, gas adsorption, carbon dioxide

1. Introduction

Carbon dioxide (CO_2) capture and storage is a key strategy to mitigate greenhouse gas emissions and combat climate change. One of the major challenges in this area is to identify cost-effective and efficient materials for CO_2 capture and storage.[1,2] Porous organic materials (POMs) have emerged as one of the most promising materials for CO_2 capture due to their high surface area, tunable functionality, and

★ Corresponding author
Phone : +964-7718932226
E-mail : emad_yousif@hotmail.com

controllable pore size.[3] POMs are organic compounds that have a highly porous structure and contain functional groups that can selectively adsorb CO_2. The design and synthesis of POMs for CO_2 capture is a rapidly growing research area, and various POMs, including porous aromatic frameworks (PAFs), porous organic polymers (POPs), and covalent organic frameworks (COFs), have been developed.[4] PAFs are a subclass of POMs that have a rigid and stable framework with a high degree of conjugation, which allows for strong interactions with CO_2 molecules.[5] PAFs have shown promising results for CO_2 capture due to their high CO_2 adsorption capacity, selectivity, and excellent stability under a wide range of conditions. POPs are another class of POMs that have tunable properties, including pore size and surface area, which can be tailored for CO_2 capture. COFs are a subclass of POMs that have a well-defined crystalline structure, and their properties can be precisely controlled by design.[6] The development of POMs for CO_2 capture has been driven by the need for highly efficient and cost-effective materials for industrial-scale CO_2 capture.[7] The conventional CO_2 capture technologies, including amine-based absorption and adsorption technologies, have several limitations, including high energy consumption, corrosion issues, and low CO_2 adsorption capacity.[8] POMs offer several advantages over conventional CO_2 capture technologies, including high CO_2 adsorption capacity, high selectivity, and low energy consumption. Additionally, POMs can be regenerated by simple processes, making them ideal for large-scale industrial applications.[9] The development of POMs for CO_2 capture is a highly interdisciplinary research area that involves the synthesis of novel materials, fundamental studies of their properties and mechanisms, and optimization of their performance for real-world applications. In recent years, several studies have reported the synthesis and characterization of novel POMs for CO_2 capture, including PAFs, POPs, and COFs. The properties of these materials have been investigated using various techniques, including X-ray diffraction (XRD), nitrogen adsorption-desorption isotherms, Fourier transform infrared spectroscopy (FTIR), and solid-state nuclear magnetic resonance (SSNMR) spectroscopy.[10,11] Despite the significant progress made in the development of POMs for CO_2 capture, several challenges remain. One of the key challenges is the optimization of the performance of POMs for real-world applications, including their stability under harsh operating conditions, their scalability, and their cost-effectiveness. Additionally, the development of POMs for CO_2 capture requires a deep understanding of the fundamental mechanisms of CO_2 adsorption and desorption, which is still an active area of research.[12,13]

Porous aromatic Schiff bases materials have gained significant attention as a promising class of materials for CO_2 capture and storage applications due to their high surface area, porosity, and chemical stability.[14,15] Porous aromatic Schiff base materials are a type of porous organic polymers that are synthesized by the condensation of aldehydes and amines under appropriate conditions.[16] These materials possess a rigid and stable framework consisting of interconnected pores and channels, which offer high surface area and high porosity. The unique chemical structure of Porous aromatic Schiff base materials provides them with a large number of adsorption sites, which can selectively bind CO_2 molecules over other gases.[17-19] Recent studies have shown that Porous aromatic Schiff base materials exhibit exceptional CO_2 sorption properties, making them a potential candidate for carbon capture applications.[20,21] Porous aromatic Schiff base materials can capture CO_2 through a range of mechanisms such as physisorption, chemisorption, and even reversible covalent bonding. Furthermore, porous aromatic Schiff base materials can be easily synthesized with tunable properties, making them highly versatile and suitable for a range of applications.[22] In this context, this study aims to investigate the potential of porous aromatic Schiff base materials as a highly effective media for CO_2 storage. The study will review the synthesis and characterization of porous aromatic Schiff base materials, their CO_2 sorption properties, and the effect of various parameters such as temperature, pressure, and gas composition on their CO_2 adsorption properties.[23,24] Overall, this study is expected to provide valuable insights into the design

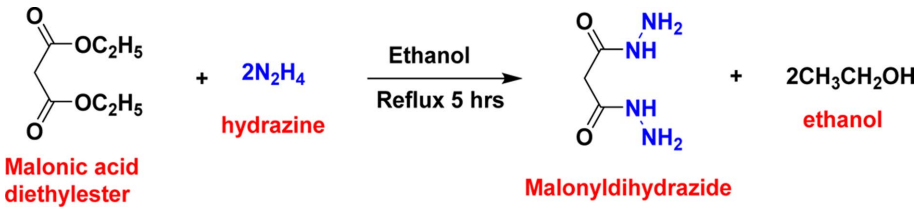

Scheme 1. Steps of preparation of malonic acid dihydrazide.

of novel materials for CO_2 capture and storage, which is a critical area of research for achieving a sustainable future.[25] The use of porous aromatic Schiff base materials as an effective media for CO_2 storage could contribute to reducing greenhouse gas emissions and mitigating climate change.[26,27] The results of this study could be useful for developing new carbon capture technologies that are cost-effective and efficient. This study, we present the utilization of Schiff bases, which are highly aromatic and porous, as an effective CO_2 capture media at 40 bars and 323 K.

2. Experimental

All chemicals utilized in this study were of the highest quality possible and were used directly from the metal chloride salts ($CoCl_2.6H_2O$, $NiCl_2.6H_2O$, $CuCl_2.2H_2O$, and $ZnCl_2$) rather than undergoing any additional purification steps.

2.1. Instrumentation

Micrometric Surface Area and Porosity Analyzers, the nitrogen adsorption-desorption isotherms for gas storage samples (Co(II), Ni(II), Cu(II), and Zn(II)) complexes of synthesized Schiff base, in Tehran Iran, were analyzed using a Micro Active for TriStar II Plus Version 2.03 micrometric analyzer. Using Barrett-Joyner-hypothesis, Halenda's analyzer determined the pore volume, diameter, and pore size distribution of the sample under investigation (BJH). Field emission scanning electron microscopy (FESEM) and gas storage of Schiff base complexes (Co(II), Ni(II), Cu(II), and Zn(II) were performed using a ZEISS system model: Sigma VP from the USA at an accelerating voltage of 10Kv. When it comes to ligand's gas storage of Schiff base complexes (Co(II), Ni(II), Cu(II), and Zn(II)), tests for EDX and mapping were conducted by Oxford Instruments, UK.

2.2. Synthesis of malonic acid di hydrazide

The first step of the ligand synthesis process includes making malonic acid di hydrazide, as explained here. Malonic acid diethylester (10 g, 0.062 mol) was dissolved in 10 ml of ethanol and left to stir at room temperature. Aqueous hydrazine (10 g, 0.25 mol) was added dropwise while being constantly stirred, then the reaction was refluxed for 6 hours before being stopped and cooled down to ambient temperature. The formed residue was filtered and the precipitate was washed with dry ether and methanol. Absolute ethanol was used to recrystallize the product giving a white precipitate 80 % yield (7.1 g), m.p. 159 °C. Malonic acid di hydrazide preparation is shown in Scheme 1.

2.3. Synthesis of Schiff base ligand (L)

In mole ratio 1:2, 2-hydroxy-1-naphthaldehyde (2.6 g, 0.015 mol) in 10 mL of methanol was added slowly with stirring to prepared malonic acid dihydrazide solution (1.0 g, 0.004 mol), in 10 mL of methanol. Then 2-3 drops of glacial acetic acid were added to the reaction mixture. The mixture was left to react under reflux conditions for 5 hr, then yellow crystals glossy precipitate was formed which was collected by filtration, washed, and recrystallized by hot ethanol. The product was dried over anhydrous $CaCl_2$ in a vacuum to give 80 % (2.88 g) yield, m.p 244 °C see Scheme 2 for the reaction Scheme.

2.4. Synthesis of Schiff base metal complexes

The copper complex was synthesized by dissolving 0.2 g, 0.001 mole of the Copper chloride dehydrate

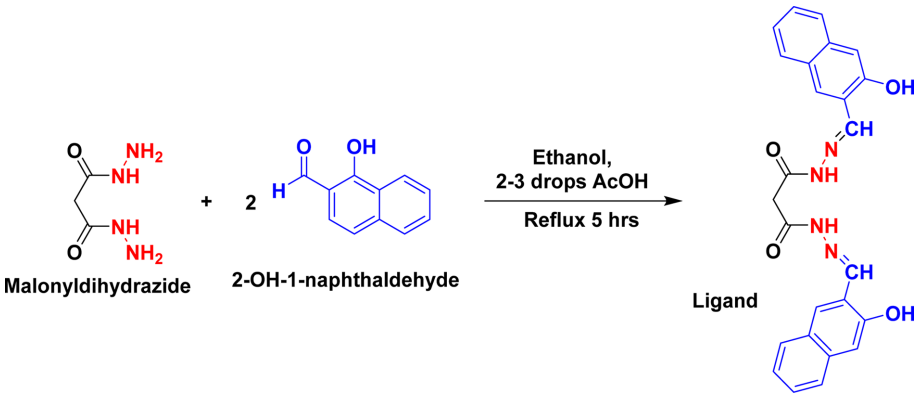

Scheme 2. Steps of Preparation of Schiff base ligand.

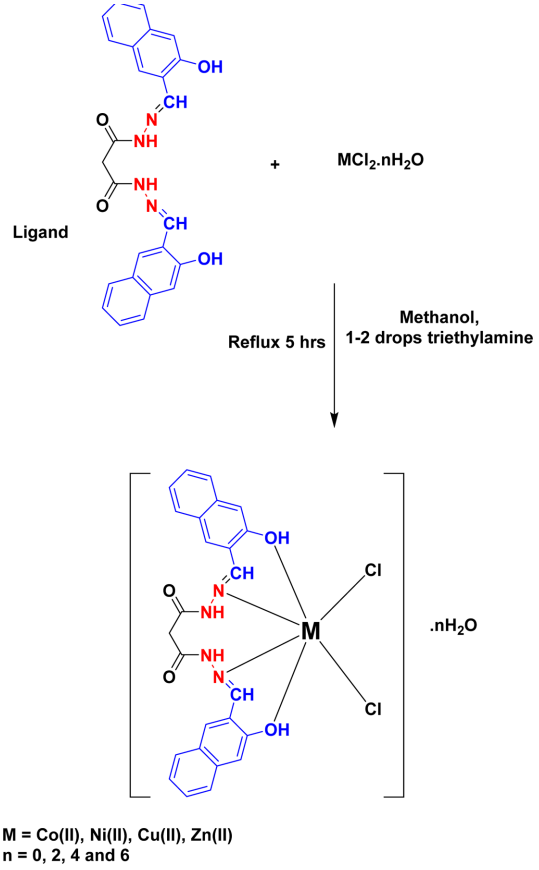

Scheme 3. Preparation of Schiff base Metal Complexes.

in 10 ml methanol and dissolving (0.5 g, 0.0001 mol) of the synthesized ligand in 10 ml of methanol with continuous stirring for about (10 min) and adding few drops of DMF to complete solubility, followed by adding the solution of the dissolved metal salt onto a solution of the dissolved ligand in the mole ratio (1:1) of (metal-ligand) and adding 1-2 drops of trimethylamine. The mixture was stirred under reflux for 5 hr until the precipitate was formed. The colored complexes were separated by filtration, washed with methanol, recrystallized, and left to dry at room temperature for 24 hours. All other complexes ($CoCl_2.6H_2O$, $NiCl_2.6H_2O$, and $ZnCl_2$) were prepared using the same procedure as shown in Scheme 3 with good to very good percentage yield see *Table* 1.

Table 1. The physical properties of the prepared compounds

Compound	Color	M.P ºC	Yield%
Ligand	Yellow	240-244	80
Cu	Dark green	>285	75
Ni	Green yellowish	258-260	70
Zn	yellow	240-248 d	83
Co	Green brownish	240-245	72

3. Results and Discussion

The ligand was synthesized in two steps firstly malonyldihydrazide was synthesized from a reaction of malonic acid with two moles of hydrazine. The crude product was purified by recrystallization from absolute ethanol. The pure product was reacted with two moles of 2-hydroxy-1-naphthaldehyde to produce the target ligand which was purified as well by recrystallization. Finally, the prepared ligand was used to synthesized five new complexes by reacting

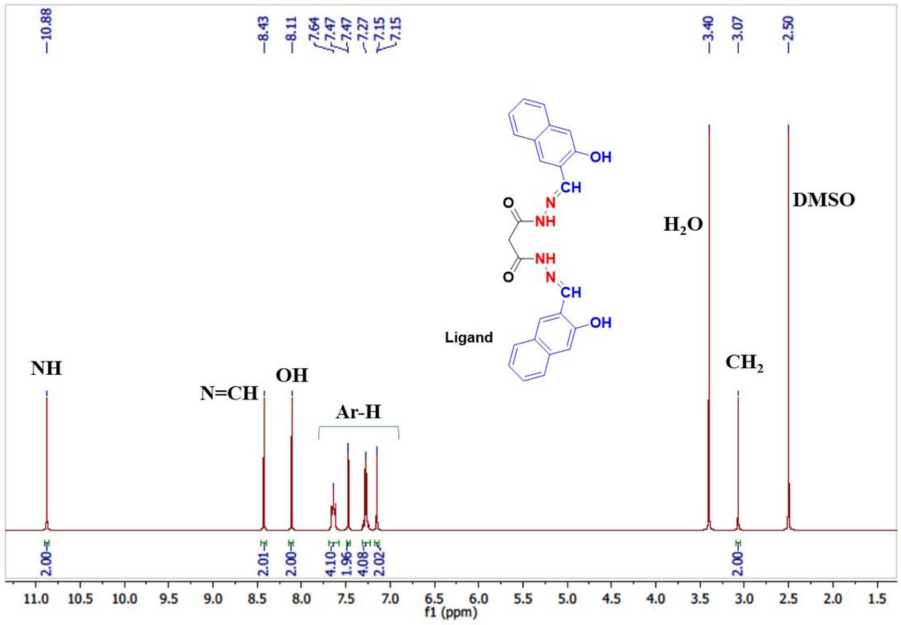

Fig. 1. ^{1}H NMR of synthesized ligand.

it with corresponding metallic chloride. The percentage yields and physical features of prepared molecules were summarized in *Table* 1. Various techniques were used to characterize the chemical structure of syn- thesized materials as will be explained in the next sections.

3.1. Characterization of Schiff Bases ligand by ^{1}H-NMR Spectroscopy

The synthesized ligand chemical structure was characterized using ^{1}H NMR spectroscopy. Hence the ^{1}H NMR spectrum shows all needed peaks at the corresponding environments, integrations, and multiplicity to demonstrate the chemical structure of the ligand. The proton of the imine group (N = CH) gives a strong sharp singlet peak at 8.43 ppm with the integration two because the structure has two symmetrical imine groups. The exchange protons of (NH and OH) groups have shown singlet peaks at chemical shifts 10.88 and 8.11 ppm. It is suggested that 10.88 ppm belongs to the NH group because it is next to the carbonyl group which causes the de-shielding of protons. On the other hand, the protons of aromatic regions show peaks at regions between 7.15 to 7.69 ppm which is the aromatic region with required integration

Table 2. ^{1}H NMR data of synthesized ligand

Compound	^{1}H-NMR
Ligand	δ = 3.07 ppm (2H, CH_2), 7.15 ppm (s, 2H, Ar-H), 7.20-7.32 ppm (m, 4H, Ar-H), 7.47 ppm (s, 2H, Ar-H), 7.60-7.69 ppm (m, 4H, Ar-H), 8.11 ppm (s, 2H, OH) from the phenolic proton, 8.43 ppm to azomethine (s, 2H, HC=N), 10.88 ppm (s, 2H, NH).

(12). Finally, the CH_2 group showed a singlet peak at the aliphatic region 3.07 ppm, this is because it is next to two carbonyl groups as shown in *Fig.* 1. From all the above, it can be said that the ligand has been synthesized successfully with a high percentage of purity. The ^{1}H NMR data of the syn- thesized ligand were summarized in *Table* 2.

3.2. Characterization of Schiff Bases ligand by ^{13}C-NMR Spectroscopy

The synthesized ligand chemical structure was characterized using ^{13}C NMR spectroscopy. Hence the ^{13}C NMR spectrum shows all needed peaks at the corresponding environments to demonstrate the chemical structure of the synthesized ligand. The carbon atom of the imine group (N = CH) gives a

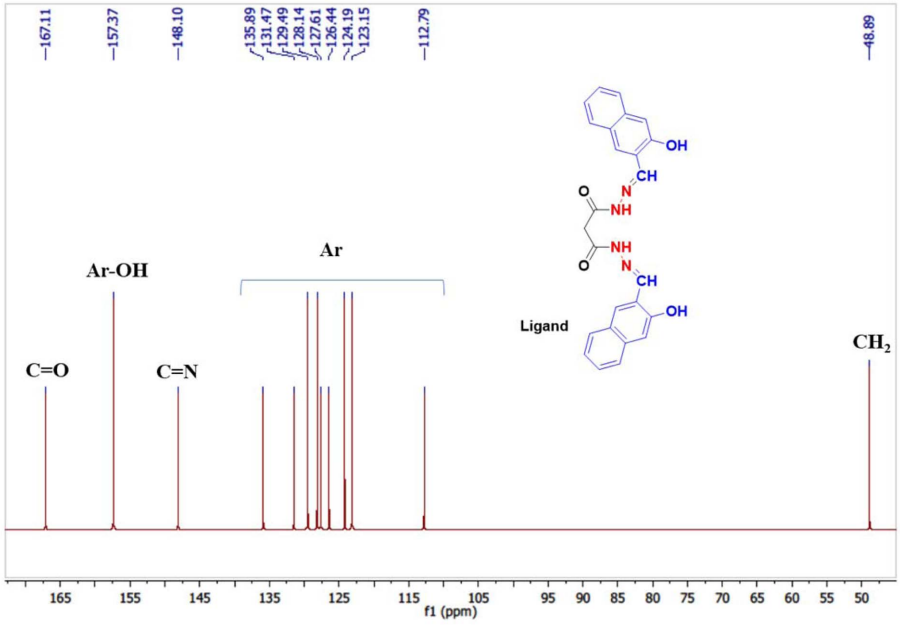

Fig. 2. ^{13}C NMR of synthesized ligand.

peak at 148.10 ppm where Schiff base groups spouse to be. On the other hand, carbonyl groups show a peak at 167.11 ppm because oxygen has a higher electronegativity than nitrogen which causes more de-shielding. However, there is still a peak above the aromatic region (157.37 ppm) which could belong to aromatic carbon atoms next to the oxygen. Thus, the carbon atoms of aromatic regions show nine peaks at regions between 112.79 to 135.89 ppm which is the aromatic region. Finally, the CH_2 group showed a peak at the aliphatic region 48.89 ppm, this is because it is next to two carbonyl groups as shown in *Fig.* 2. From all the above, it can be said that the ligand has been synthesized successfully with a high percentage of purity. The ^{13}C NMR data of the synthesized ligand were summarized in *Table* 3.

Table 3. ^{13}C NMR data of synthesized ligand

Compound	^{13}C-NMR
Ligand	δ = 48.89 ppm (1C, CH_2), 112.79, 123.15, 124.19, 126.44, 127.61, 128.14, 129.49, 131.47, 135.89 ppm (18C, Ar naphthalene), 148.10 ppm (2C, CH=N azomethine group), 157.37 ppm (2C, Ar-OH) and 167.11 ppm (2C, C=O carbonyl group).

3.3. Characterization of Schiff Bases ligand and its complexes by FTIR

Fourier Transform Infrared Spectroscopy is a valuable method to determine the functional groups and the creation of new bands in the manufactured compounds. *Table* 4 reports the FTIR spectroscopy results for the ligand and their produced complexes. *Figs.* 3-7 shows

Table 4. FTIR Spectroscopy Measurements of ligand, and its Complexes

Compound	O-H Phenol	N-H	C-H Ar	C-H Alp	C=O	C=N	C=C	M-N	M-Cl
Ligand	3409	3330	3109	2889	1700	1613	1596	---	---
Co(II)	3479	3355	3110	2893	1702	1623	1598	422	351
Ni(II)	3450	3203	3186	2896	1701	1623	1539	422	333
Cu(II)	3461	3423	3109	2925	1704	1621	1542	420	351
Zn(II)	3479	3359	3053	2925	1703	1620	1577	476	352

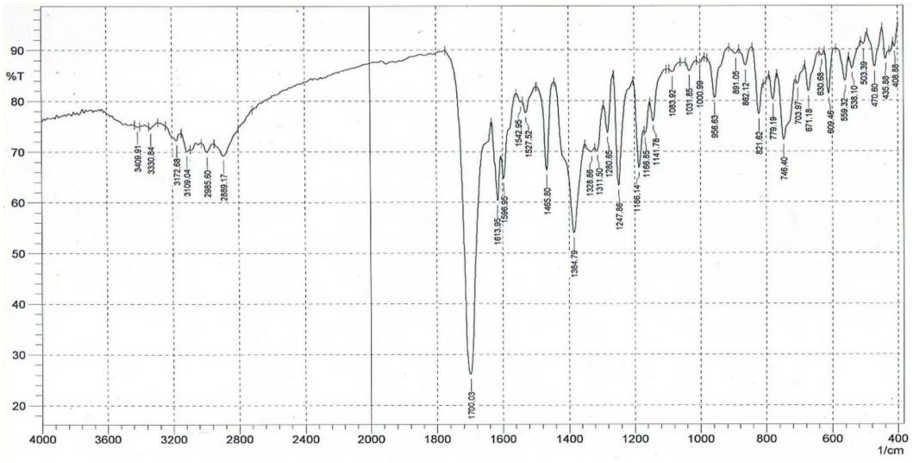

Fig. 3. FTIR-Spectrum of Schiff Base ligand.

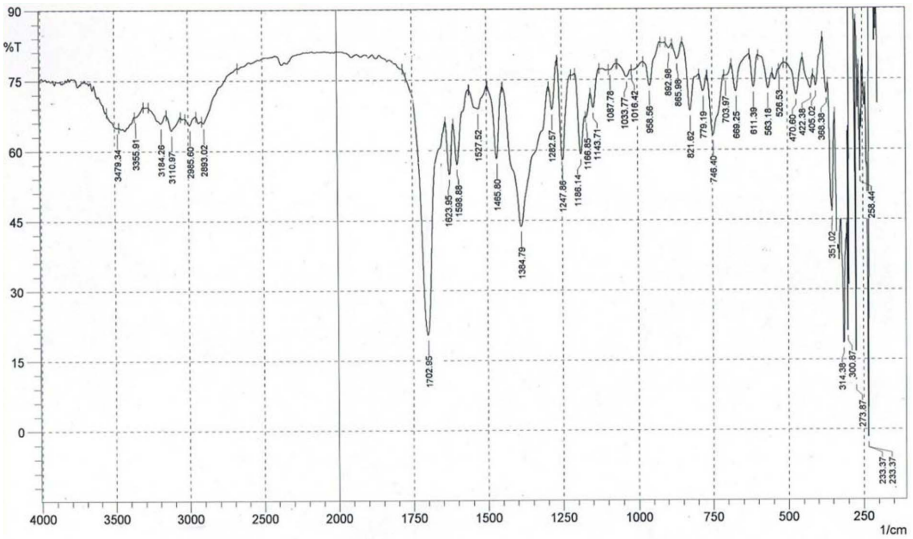

Fig. 4. FTIR-Spectrum of Co(II) complex.

the FTIR spectrums of synthesized ligand and its complexes.

The tetradentate Schiff base ligand displays a sharp band at 3109 cm^{-1}, and 1596 cm^{-1} assigned to ν(C-H)Ar, and ν(C = C) respectively.[28] A strong band appeared at 1613 cm^{-1} assigned to the stretching band of the azomethine group. The coordination of the metal ions to the nitrogen azomethine leads to a shift-up in the frequency of ν(C = N) value due to the decreases in the electron density on the azomethine after donating electrons of nitrogen to the partially filled d-orbitals of the metal ions(II).[29] The IR-spectra of the complexes, exhibit characteristic bands around (1613-1623) cm^{-1} showing that the metal ions coordinate to the ligand via the azomethine nitrogen atom.[30] The stretching vibrations of the phenolic hydroxyl group cause a large band at 3409-3479 cm^{-1} in the IR spectra of the ligands. Intermolecular hydrogen bonding between the phenolic and azomethine groups accounts for the broadness. New stretching modes were observed in the far-infrared spectra of the complexes that didn't exist in the spectrum of ligand at (420-476) cm^{-1}, (526-563), and (327-352) cm^{-1} which are attributed to υ (M-N), υ (M-O) and

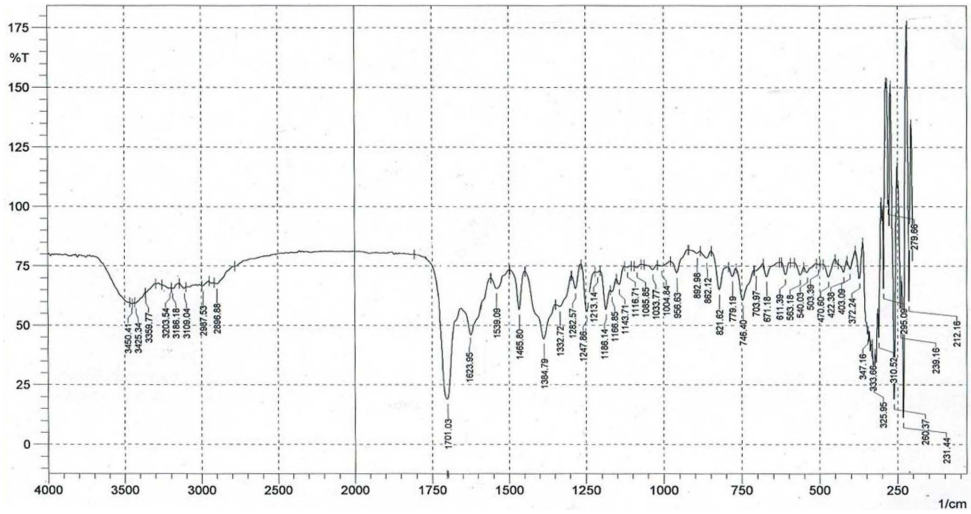

Fig. 5. FTIR-Spectrum of Ni(II) Complex.

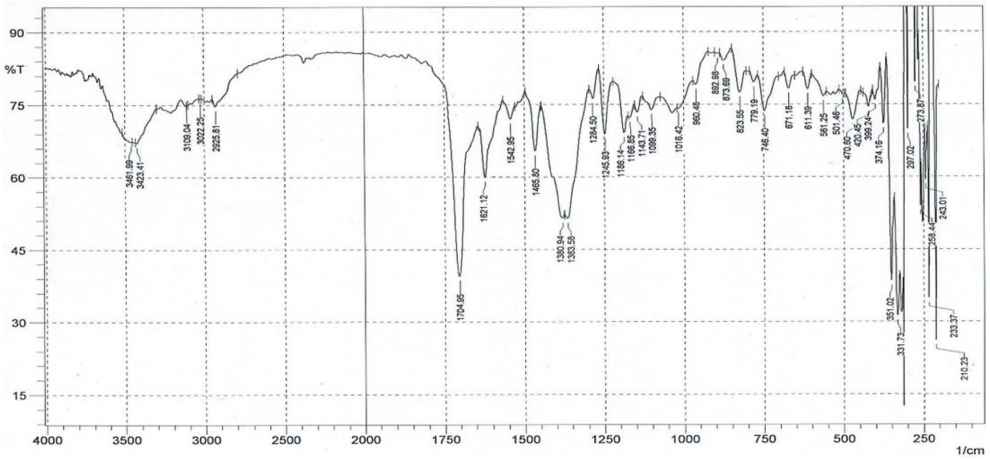

Fig. 6. FTIR-Spectrum of Cu(II) Complex.

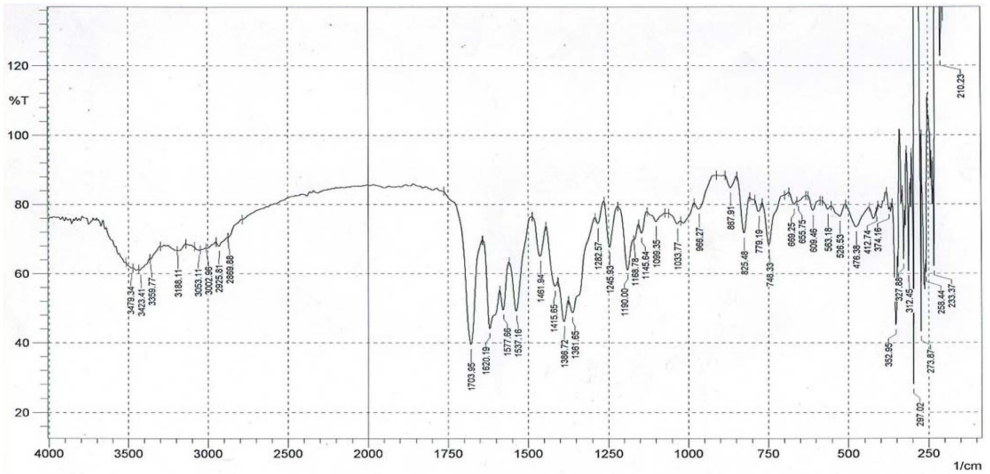

Fig. 7. FTIR-Spectrum of Zn(II) Complex

υ (M-Cl) as evidence on the formation bonds between the metal ions(II) and the nitrogen azomethine, hydroxyl group and chloride, respectively.

3.4. Energy dispersive X-ray (EDX) Analysis of Synthesized Schiff base Complexes

Energy dispersive X-ray (EDX) was used for

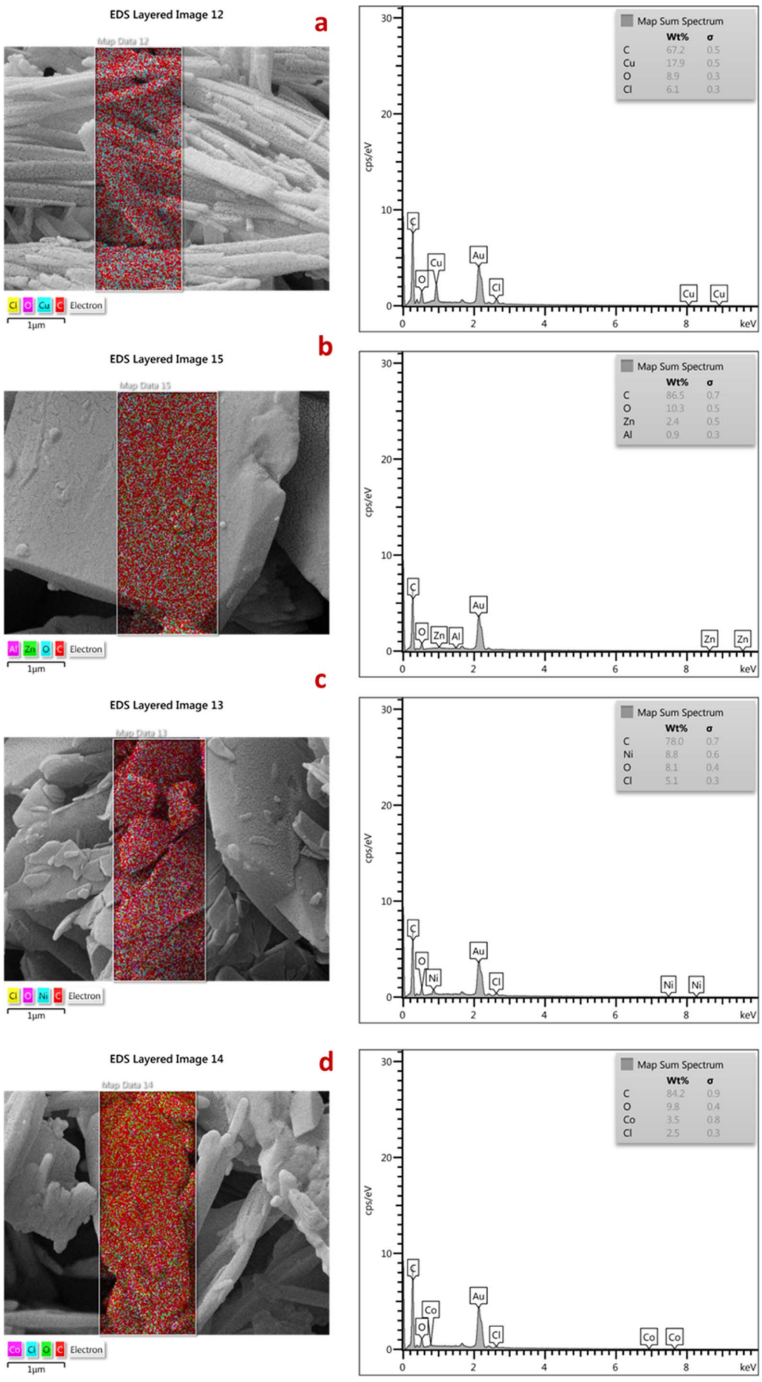

Fig. 8. EDX graphs of (a) Cu(II), (b) Zn(II), (c) Ni(II), and (d) Co(II) complexes.

synthetic Schiff base complexes to offer details on the elemental composition of solid surfaces.[31] Field emission scanning electron microscopy (FESEM), a standard chemical microanalysis technique, and EDX are coupled to derive the chemical formula of produced compounds. The EDX mapping of the complexes, as seen in *Fig.* 8, reveals the elemental chemical compositions of the produced complexes.

3.5. Inorganic complexes as gas storage materials

3.5.1. Surface area determination

Complexes were subjected to 77 K nitrogen gas adsorption and desorption experiments using a surface area measuring equipment. By using the Brunauer, Emmett, and Teller (BET) approach, specific surface areas of complexes were measured and gas volume-relative pressure isotherms were generated. The "nitrogen adsorption method", which made it easier to analyze micro-, meso-, and macropore sizes and specific surface areas of the pores, yielded complicated pore diameters and sizes, which were presented in *Table* 5 and *Fig.* 9-12.

According to categorization in The International Union of Pure and Applied Chemistry (IUPAC), which correlates to meso pore size generally, results in *Table* 4 reveal the typical pore diameter is in the 2 to 50 nm range. According to *Table* 5, rather than the size of the particular pore volume, the size of a specific surface area is dependent on the size of the pores. Because the wall surface area increases with decreasing pore size of used materials. Additionally, it was shown that the specific surface area and pore volume were connected to the complexes' structure and adsorption capacity.[32] There were no monolayers and only very weak interactions between the gas and adsorbents, as shown by the type III isotherms seen

Table 5. Surface area and pore size distribution of metal complexes obtained by N_2 Adsorption

Complex	S_{BET} (m^2/g)	Pore volume (cm^3/g)	Average pore diameter (nm)
Co(II)	4.7	0.02	16.9
Ni(II)	6.2	0.04	29.3
Zn(II)	8.7	0.028	12.8
Cu(II)	19	0.07	15

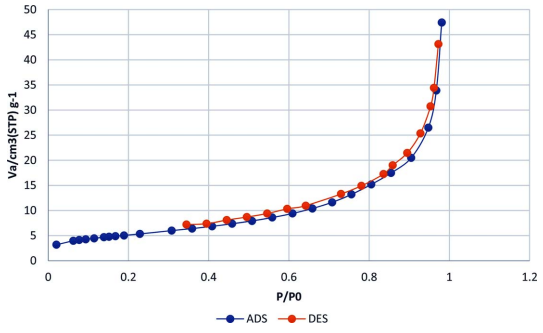

Fig. 9. N_2 Adsorbed isotherm of Co(II) complex.

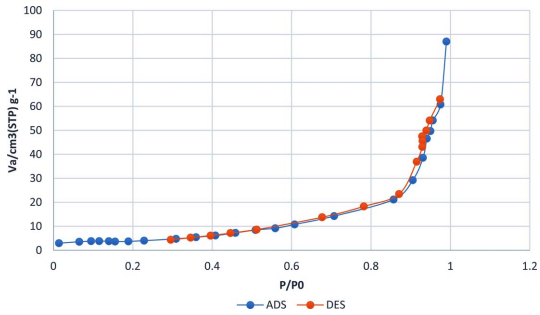

Fig. 10. N_2 Adsorbed isotherm of Ni(II) complex.

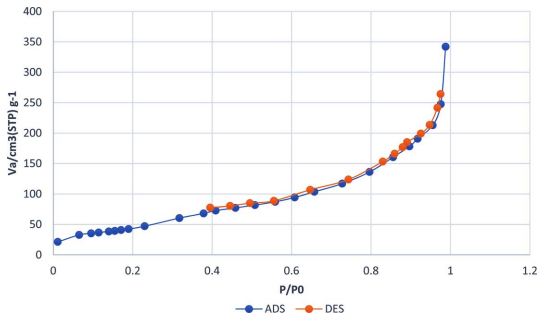

Fig. 11. N_2 Adsorbed isotherm of Zn(II) complex.

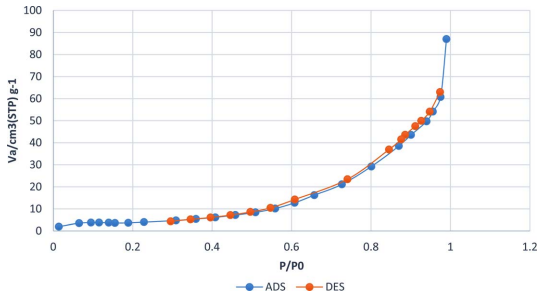

Fig. 12. N_2 Adsorbed isotherm of Cu(II) Complex.

in (*Fig.* 2, *Fig.* 3, *Fig.* 4 and *Fig.* 5). The fact that the isotherms began at the origin indicates that the heat of adsorption and condensation were equivalent in intensity. Positive CO_2 gas adsorption on the surface of metal complexes resulted in a significant rise in adsorption as the pressure rose.[33,34] The potency and effectiveness of metal complexes in gas storage are enhanced by the strong stacking interactions, which also regulate the 2D solid-state packing and obstruct interpenetration, according to measurements of CO_2 gas sorption at high pressures (up to 40 bar).

3.5.2. FESEM of metal complexes

The FESEM method was used to assess the morphology, porosity, and particle size of the produced Schiff base Co(II), Ni(II), Cu(II), and Zn(II) complexes. Images produced by the FESEM demonstrate superb resolution, clarity, and minimal distortion of the investigated particles.[35,36] Schiff base complexes' homogeneous, amorphous, and rough surfaces are exposed in *Fig.* 13-16, and these characteristics make them an ideal surface for CO_2 gas extraction. The complexes' images show minute particles creating various shapes and sizes through homogeneous agglomeration. According to the IUPAC pores classifications,[37] the FESEM pictures indicate that the compounds have a mesoporous structure, supporting the findings of the BJH method. Macro-pores are those with a diameter more than 50 nm, Meso-pores have pores that range in size from 2 nm to 50 nm, and Micro-pores are those with a diameter of under 2 nm.

The sorption of porous aromatic Schiff base complexes (Co(II), Ni(II), Zn(II), and Cu(II)) was studied at fixed pressure and temperature 50 bars and

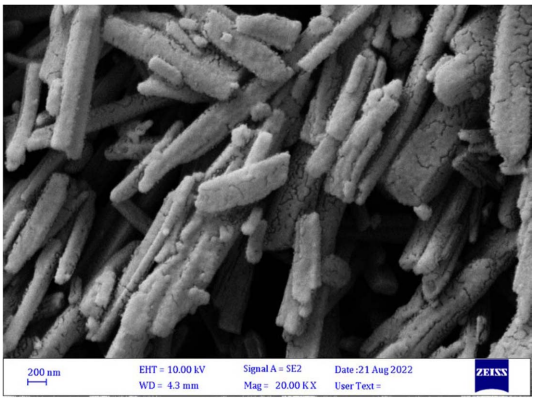

Fig. 13. Field emission scanning electron microscopy (FESEM) image of Cu(II) complex.

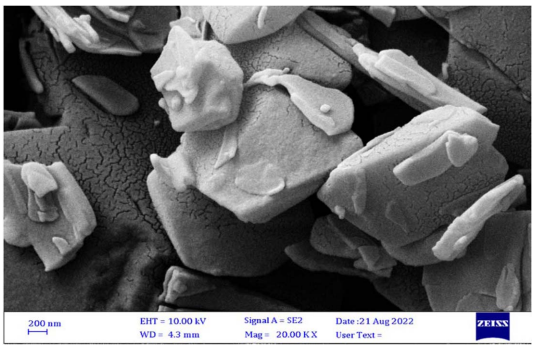

Fig. 14. Field emission scanning electron microscopy (FESEM) image of Ni(II) complex.

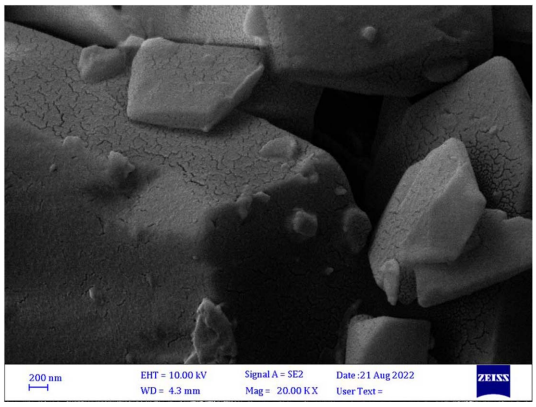

Fig. 15. Field emission scanning electron microscopy (FESEM) image of Zn(II) complex.

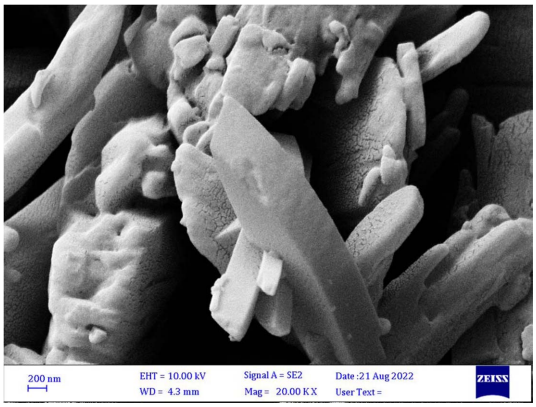

Fig. 16. Field emission scanning electron microscopy (FESEM) image of Co(II) complex.

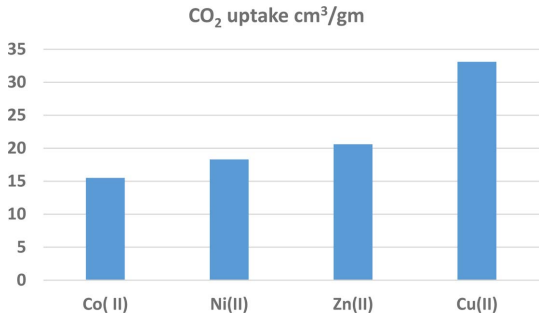

Fig. 17. CO_2 adsorption isotherms of metal complexes.

Table 6. CO_2 capacity for metal complexes

Complex	CO_2 uptake $cm^3.gm^{-1}$
Co(II)	15.5
Ni(II)	18.3
Zn(II)	20.6
Cu(II)	33.1

323 K. *Fig.* 17 shows the adsorption isotherms of CO_2 on metal complexes and the gases uptakes are recorded in *Table* 6.

Because they have a high capacity to create van der Waals and dipole-dipole interactions between the adsorbent and adsorbate, porous aromatic Schiff base complexes (Co(II), Ni(II), Zn(II), and Cu(II)) exhibited the effectiveness of CO_2 adsorption. According to *Fig.* 17, the CO_2 adsorption capacities for Co(II), Ni(II), Zn(II), and Cu(II) complexes, respectively, were 15.5, 18.3, 20.6, and 33.1 cm^3/g. Evidently, when compared to the other investigated compounds, Cu(II)) complex showed the greatest efficiency of CO_2 adsorption capacity. Other ways to boost adsorption effectiveness include strong dipole-dipole interactions and heteroatoms found inside molecules. Therefore, porous materials with oxygen and nitrogen atom units are efficient at trapping CO_2 gas in a specific manner.

4. Conclusions

In conclusion, Carbon Dioxide (CO_2) storage is a crucial challenge faced by the scientific community today, and extensive research is being carried out to find a viable solution to this issue. One of the promising approaches is the use of porous aromatic Schiff Bases as a highly effective media for CO_2 storage and studied the influence of their morphologies. This technology has shown impressive results in CO_2 adsorption and storage, and it is an excellent alternative to traditional methods of CO_2 storage. All spectral data from this investigation showed that the produced Schiff base compound acted as a tetra dentate ligand, attaching to the metal ion via the phenolic oxygen and the azomethine nitrogen. The analytical results also showed that the M:L ratio is 1:1 in all the produced complexes, which is consistent with a mononuclear structure. porous aromatic Schiff Bases offer a high surface area and tunable chemical properties, which make them ideal for CO_2 adsorption. Furthermore, their porous structure allows for the trapping and storage of CO_2 molecules, leading to a reduction in greenhouse gas emissions. The application of this technology can potentially lead to the development of cost-effective, energy-efficient, and environmentally friendly solutions to tackle the issue of CO_2 storage. In summary, the use of porous aromatic Schiff Bases as a highly effective media for CO_2 storage is a promising area of research that holds significant potential for addressing the problem of climate change. Further research and development in this field is necessary to refine the technology and make it more practical for widespread use.

Conflict of Interest

The authors declare no conflict of interest.

References

1. G. Zeng, Y. Zhang, L. Li, Y. Huang, M. Li, and C. Yan, *Journal of Materials Chemistry A*, **8**(7), 3223-3244 (2020). DOI: 10.4324/9780429448935
2. J. Wang, Y. Wang, H. Hu, Q. Yang, and J. Cai, *Nanoscale*, **12**(7), 4238-4268 (2020). https://doi.org/10.1039/C9NR09697C
3. J. Du, H. Ouyang, and B. Tan, *Chemistry-An Asian Journal*, **16**(23), 3833-3850 (2021). https://doi.org/10.1002/

asia.202100991

4. G. Ji, Y. Zhao, and Z. Liu, *Green Chemical Engineering*, **3**(2), 96-110 (2022). https://doi.org/10.1016/j.gce.2021.11.011
5. F. Tang, J. Hou, K. Liang, J. Huang, and Y. N. Liu, *European Journal of Inorganic Chemistry*, **37**, 4175-4180 (2018). https://doi.org/10.1002/ejic.201800764
6. P. Bhanja, A. Modak, and A. Bhaumik, *ChemCatChem*, **11**(1), 244-257 (2019). https://doi.org/10.1002/cctc.201801046
7. X. Wu, R. Guan, W. T. Zheng, K. Huang, and F. Liu, *Journal of Materials Science*, **56**, 9315-9329 (2021). https://doi.org/10.1007/s10853-021-05835-z
8. L. Zou, Y. Sun, S. Che, X. Yang, X. Wang, M. Bosch, Q. Wang, H. Li, M. Smith, S. Yuan, and Z. Perry, *Advanced Materials*, **29**(37), 1700229 (2017). https://doi.org/10.1002/adma.201700229
9. N. Kundu and S. Sarkar, *Journal of Environmental Chemical Engineering*, **9**(2), 105090 (2021). https://doi.org/10.1016/j.jece.2021.105090
10. J. Chen, L. Jiang, W. Wang, Z. Shen, S. Liu, X. Li, and Y. Wang, *Journal of Colloid and Interface Science*, **609**, 775-784 (2022). https://doi.org/10.1016/j.jcis.2021.11.091
11. A. Chowdhury, S. Bhattacharjee, R. Chatterjee, and A. Bhaumik, *Journal of CO_2 Utilization*, **65**, 102236 (2022). https://doi.org/10.1016/j.jcou.2022.102236
12. K. Huang, J.Y. Zhang, F. Liu, and S. Dai, *Acs Catalysis*, **8**(10), 9079-9102 (2018). https://doi.org/10.1021/acscatal.8b02151
13. D. Luo, T. Shi, Q. Li, Q. Xu, M. Strömme, Q. F. Zhang, and C. Xu, *Angewandte Chemie International Edition*, **62**, e202305225 (2023). https://doi.org/10.1002/anie.202305225
14. T. T. Liu, J. Liang, Y. B. Huang, and R. Cao, *Chemical Communications*, **52**(90), 13288-13291 (2016). https://doi.org/10.1039/c6cc07662a
15. Z. Yuan, M. R. Eden, and R. Gani, *Industrial & Engineering Chemistry Research*, **55**(12), 3383-3419 (2016). https://doi.org/10.1021/acs.iecr.5b03277
16. Y. Li, C. Zhang, X. Li, and H. Jiang, *Journal of Materials Chemistry A*, **7**(24), 14309-14324 (2019). https://doi.org/10.1039/C9CP06925A
17. A. A. Yaseen, E. T. Al-Tikrity, G. A. El-Hiti, D. S. Ahmed, M. A. Baashen, M. H. Al-Mashhadani, and E. Yousif, *Processes*, **9**(4), 707 (2021). https://doi.org/10.3390/pr9040707
18. Y. Wang, C. Kang, Z. Zhang, A. K. Usadi, D. C. Calabro, L. S. Baugh, Y. D. Yuan, and D. Zhao. *ACS Sustainable Chemistry & Engineering*, **10**(1), 332-341 (2021). https://doi.org/10.1021/acssuschemeng.1c06318
19. M. G. Rabbani, A. K. Sekizkardes, O. M. El-Kadri, B. R. Kaafarani, H. M. El-Kaderi. *Journal of Materials Chemistry*, **22**(48), 25409-25417 (2012). https://doi.org/10.1039/C2JM34922A
20. M. S. B. Reddy, D. Ponnamma, K. K. Sadasivuni, B. Kumar, and A. M. Abdullah,. *RSC Advances*, **11**(21), 12658-12681 (2021). https://doi.org/10.1039/D0RA10902A
21. A. Rehman and S. J. Park, *Journal of CO_2 Utilization*, **21**, 503-512 (2017). https://doi.org/10.1016/j.jcou.2017.08.016
22. W. Xie, D. Cui, S. R. Zhang, Y. H . Xu, and D. L. Jiang, *Materials Horizons*, **6**(8), 1571-1595 (2019). https://doi.org/10.1039/C8MH01656A
23. R. M. Omer, E. T. B. Al-Tikrity, G. A. El-Hiti, M. F. Alotibi, D. S. Ahmed, and E. Yousif, *Processes*, **8**, (2020). https://doi.org/10.3390/pr8010017
24. B. Dziejarski, J. Serafin, K. Andersson, and R. Krzyżyńska, *Materials Today Sustainability*, **24**, 100483 (2023). https://doi.org/10.1016/j.mtsust.2023.100483
25. M. N. Anwar, N. F. Fayyaz, M. F. Sohail, M. Khokhar, W. D. Baqar, K. Khan, K. Rasool, M. Rehan, and A. S. Nizami. *Journal of Environmental Management* **226**, 131-144 (2018). https://doi.org/10.1016/j.jenvman.2018.08.009
26. T. Saleh, E. Yousif, E. Al-Tikrity, D. Ahmed, M. Bufaroosha, M. Al-Mashhadani, and A. Yaseen, *Materials Science for Energy Technologies*, **5**, 344-352 (2022). https://doi.org/10.1016/j.mset.2022.08.002
27. D. S. Ahmed, G. A. El-Hiti, E. Yousif, A. A. Ali, and A. S. Hameed. *Journal of Polymer Research*, **25**, 1-21, (2018). https://doi.org/10.1007/s10965-018-1474-x
28. N. Emad, G.A . El-Hiti, E. Yousif, D. S. Ahmed, and B. M. Kariuki, *Results in Chemistry*, **6**, 101137 (2023). https://doi.org/10.1016/j.rechem.2023.101137
29. N. Emad, G. A. El-Hiti, E. Yousif, D. S. Ahmed, M. Fadhil, and B. M. Kariuki, *Results in Chemistry*, **6**, 101099 (2023). https://doi.org/10.1016/j.rechem.2023.101099
30. D. S. Ahmed, G. A. El-Hiti, E. Yousif, A. S. Hameed, and M. Abdalla. *Polymers*, **9**, 336 (2017). https://doi.org/10.3390/polym9080336

31. Z. N. Mahmood, M. Alias, E. Yousif, S. Baqer, M. Kadhom, D. Ahmed, A. Ahmed, A. Husain, M. Yusop, and A. Jawad, A. *Pollution*, **9**(2), 693-701 (2023). https://doi.org/10.22059/poll.2022.348855.1632
32. A. A. Yaseen, E. Yousif, E. T. Al-Tikrity, M. Kadhom, M. Yusop, and D. S. Ahmed. *Pollution*, **8**(1), 239-248 (2022). doi: 10.22059/poll.2021.328835.1161
33. O. G. Mousa, E. Yousif, A. A. Ahmed, G. A. El-Hiti, M. H. Alotaibi, and D. S. Ahmed. *Applied Petrochemical Research*, **10**, 157-164 (2020). https://doi.org/10.1007/s13203-020-00255-7
34. S. H. Mohamed, A. S. Hameed, E. Yousif, M. H. Alotaibi, D. S. Ahmed, and G. A. El-Hiti, *Processes*, **8**, 1488 (2022). https://doi.org/10.3390/pr8111488
35. O. Erdem and E. Yildiz, *Inorganica Chimica Acta*, **438**, 1-4 (2015). https://doi.org/10.1016/j.ica.2015.08.015
36. S. Sansul, E. Yousif, D. S. Ahmed, G. A. El-Hiti, B. M. Kariuki, H. Hashim, and A. Ahmed. *Polymers* **15**(14), 2989 (2023). https://doi.org/10.3390/polym15142989
37. S. A. Mahdi, A. A. Ahmed, E. Yousif, D. Ahmed, M. H. Al-Mashhadani, and M. Bufaroosha. *Materials Science for Energy Technologies*, **5**, 197-207 (2022). https://doi.org/10.1016/j.mset.2022.02.002

Authors' Positions

Rehab Hammoda : Lecturer
Naser Shaalan : Professor
Mohammed H. Al-Mashhadani : Assistant Professor
Dina S. Ahmed : Lecturer
Rahimi M. Yusop : Professor
Ali H. Jawad : Professor
Emad Yousif : Professor